# Sensitization to the Lysosomal Cell Death Pathway by Oncogene-Induced Down-regulation of Lysosome-Associated Membrane Proteins 1 and 2

Nicole Fehrenbacher,[1] Lone Bastholm,[2] Thomas Kirkegaard-Sørensen,[1] Bo Rafn,[1] Trine Bøttzauw,[1] Christina Nielsen,[1] Ekkehard Weber,[3] Senji Shirasawa,[4] Tuula Kallunki,[1] and Marja Jäättelä[1]

[1]Apoptosis Department and Centre for Genotoxic Stress Response, Institute for Cancer Biology, Danish Cancer Society; [2]Institute of Molecular Pathology, Faculty of Health Sciences, University of Copenhagen, Copenhagen, Denmark; [3]Institute of Physiological Chemistry, Medical Faculty, Martin-Luther-University Halle-Wittenberg, Halle, Germany; and [4]Department of Cell Biology, School of Medicine, Fukuoka University, Fukuoka, Japan

## Abstract

**Expression and activity of lysosomal cysteine cathepsins correlate with the metastatic capacity and aggressiveness of tumors. Here, we show that transformation of murine embryonic fibroblasts with *v-H-ras* or *c-src*$^{Y527F}$ changes the distribution, density, and ultrastructure of the lysosomes, decreases the levels of lysosome-associated membrane proteins (LAMP-1 and LAMP-2) in an extracellular signal-regulated kinase (ERK)- and cathepsin-dependent manner, and sensitizes the cells to lysosomal cell death pathways induced by various anticancer drugs (i.e., cisplatin, etoposide, doxorubicin, and siramesine). Importantly, *K-ras* and *erbb2* elicit a similar ERK-mediated activation of cysteine cathepsins, cathepsin-dependent down-regulation of LAMPs, and increased drug sensitivity in human colon and breast carcinoma cells, respectively. Notably, reconstitution of LAMP levels by ectopic expression or by cathepsin inhibitors protects transformed cells against the lysosomal cell death pathway. Furthermore, knockdown of either *lamp1* or *lamp2* is sufficient to sensitize the cells to siramesine-induced cell death and photo-oxidation–induced lysosomal destabilization. Thus, the transformation-associated ERK-mediated up-regulation of cysteine cathepsin expression and activity leads to a decrease in the levels of LAMPs, which in turn contributes to the enhanced sensitivity of transformed cells to drugs that trigger lysosomal membrane permeabilization. These data indicate that aggressive cancers with high cysteine cathepsin levels are especially sensitive to lysosomal cell death pathways and encourage the further development of lysosome-targeting compounds for cancer therapy.** [Cancer Res 2008;68(16):6623–33]

## Introduction

Lysosomes are highly dynamic cytosolic organelles that receive membrane traffic input from the biosynthetic (*trans*-Golgi network), endocytic, and autophagic pathways (1, 2). They contain more than 50 hydrolases that can process all the major macromolecules of the cell to breakdown products available for metabolic reuse (3, 4). Cathepsin proteases are among the best-studied lysosomal hydrolases. They are maximally active at the acidic pH of lysosomes (pH 4–5). However, many of them can be active at the neutral pH outside lysosomes, albeit with a decreased efficacy and/or altered specificity (5). For example, transformation and tumor environment enhance the expression of lysosomal cysteine cathepsins and increase their secretion into the extracellular space (6). Once outside the tumor cells, cathepsins stimulate angiogenesis, tumor growth, and invasion in murine cancer models, thereby enhancing cancer progression (7, 8). On the other hand, the leakage of cathepsins into the cytosol can trigger either necrotic or apoptotic cell death pathways (4, 9). Thus, the maintenance of lysosomal membrane integrity is of utmost importance for the cell survival.

Cancer cells harbor several acquired changes that help them to avoid spontaneous and therapy-induced apoptosis (10, 11). Thus, the lysosomal cell death pathways characterized by an early lysosomal membrane permeabilization and the subsequent translocation of cathepsins into the cytosol have awoken increasing interest among cancer researchers. Such lysosomal cell death pathways can be induced by death receptors of tumor necrosis factor (TNF) receptor family, p53 tumor suppressor protein, oxidative stress, microtubule-stabilizing and microtubule-destabilizing agents, siramesine, etoposide, staurosporine, etc. (12–19). Once in the cytosol, cathepsins, particularly cysteine cathepsins B and L and aspartate cathepsin D, can initiate the intrinsic apoptosis pathway possibly via a cleavage-mediated activation of proapoptotic Bcl-2 family proteins (20). Importantly, cytosolic cathepsins can also trigger caspase-independent and Bcl-2–insensitive cell death pathways even in highly apoptosis-resistant cancer cells (4, 21). For example, siramesine, a promising anticancer drug presently under preclinical development, is a lysosomotropic detergent that accumulates in lysosomes and directly destabilizes them, leading to the translocation of cathepsins into the cytosol- and cathepsin-dependent cell death pathway even in the presence of the antiapoptotic Bcl-2 protein (17, 22). The signaling pathways leading to the lysosomal leakage induced by most other lysosome-destabilizing agents are poorly understood. Depending on the cell type, TNF-induced permeabilization of lysosomes and the following cell death can occur either independent of caspases or via a pathway involving both caspase-8 and caspase-9 (13, 18). Free radicals, sphingosine, iron, phospholipases, and cathepsin B are among the suggested caspase-independent mediators of the lysosomal destabilization (4, 9, 23).

**Note:** Supplementary data for this article are available at Cancer Research Online (http://cancerres.aacrjournals.org/).

Current address for N. Fehrenbacher: Departments of Medicine, Cell Biology and Pharmacology, New York University Cancer Institute, New York, NY 10016.

**Requests for reprints:** Marja Jäättelä, Apoptosis Department and Centre for Genotoxic Stress Response, Institute for Cancer Biology, Danish Cancer Society, DK-2100 Copenhagen, Denmark. Phone: 45-35257318; Fax: 45-35257721; E-mail: mj@cancer.dk.



doi:10.1158/0008-5472.CAN-08-0463

Our recent data show that immortalization and oncogene-driven transformation lead to increased sensitivity to the lysosomal cell death pathways induced by TNF or siramesine (17, 24). The aim of this study was to enlighten the molecular mechanism responsible for the oncogene-mediated sensitization. For this purpose, we used four cellular transformation models, that is, NIH3T3 murine embryonic fibroblasts transformed either with (*a*) viral Harvey *ras* (*v-H-ras*) or (*b*) oncogenic *c-src*$^{Y527F}$ compared with vector-transduced cells (24), (*c*) human HCT116 colon carcinoma cells that harbor an activating mutation at codon 13 of *K-ras* compared with HCT116-derived Hkh2 cells, in which activated *K-ras* has been disrupted by homologous recombination (25), and (*d*) human MCF-7 breast carcinoma cells expressing tetracycline-regulated $NH_2$-terminally truncated active form of ErbB2 receptor tyrosine kinase (26). Prompted by our data showing that oncogenes sensitized cells to treatments that trigger lysosomal leakage by different mechanisms, we hypothesized that this sensitization was due to changes in lysosomes themselves rather than in signaling pathways that lead to the lysosomal permeabilization. Thus, we studied the effects of transformation on lysosomal density, composition, and ultrastructure and observed consistent extracellular signal-regulated kinase (ERK)-dependent increase in cysteine cathepsin expression and activity and cathepsin-dependent down-regulation of lysosome-associated membrane proteins (LAMP-1 and LAMP-2) in transformed cells. Studies using RNA interference–mediated down-regulation and ectopic expression of *lamp1* and/or *lamp2* indicated that down-regulation of *lamp1* and *lamp2* is essential, but not sufficient, to the transformation-associated sensitization to TNF and anticancer drugs.

## Materials and Methods

**Cell culture and treatments.** NIH3T3 fibroblasts, HCT116 colon carcinoma cells, and HCT116-derived Hkh2 cells (25) were propagated in DMEM with GlutaMAX (Invitrogen) supplemented with 10% heat-inactivated FCS, 0.1 mmol/L nonessential amino acids (Invitrogen), and antibiotics. NIH3T3 cells were transduced with an empty *pBabe-puro* retrovirus (provided by Christian Holmberg, University of Copenhagen, Copenhagen, Denmark) or *pBabe-puro* encoding for *v-H-ras* (provided by N. Dietrich, University of Copenhagen), *c-src*$^{Y527F}$ (provided by S. Courtneidge, Van Andel Research Institute, Grand Rapids, MI), *H-ras-V12* and its dominantly active effector loop mutants *35S, 37G*, and *40C* (provided by Channing Der, University of North Carolina, Chapel Hill, NC; ref. 27), or *lamp-2* (Supplementary Data) as described previously (24). Cells were used at passages 3 to 10 after transduction. U-2-OS osteosarcoma and MCF-7-tet-ΔNErbB2 cells (26) were cultured in RPMI 1640 with GlutaMAX and 6% heat-inactivated FCS. The medium for MCF-7-tet-ΔNErbB2 cells was further supplemented with 0.3 μg/mL tetracycline (Sigma-Aldrich).

Siramesine {1′-[4-[1-(4-fluorophenyl)-1*H*-indol-3-yl]-1-butyl]spiro[isobenzo furan-1(3*H*),4′-piperidine]} was kindly provided by Christian Thomsen (Lundbeck A/S, Valby, Denmark); recombinant murine TNF was purchased from R&D Systems; etoposide, cisplatin, doxorubicin hydrochloride, concanamycin A (ConA), and cycloheximide were from Sigma-Aldrich; zFA-fmk was from Enzyme System Products; Ca-074-Me was from Peptides International; DEVD-cmk was from Bachem; U0126 was from Promega; and PD98059 was from Calbiochem.

**RNA interference.** The cells were transfected with Oligofectamine or RNAiMax (Invitrogen) and 6 to 25 nmol/L of small interfering RNA (siRNA) according to the manufacturer's guidelines. siRNAs targeting *ctsb* encoding for cathepsin B (5′-UUGUCCAGAAGUUCCAAGCUUCAGC-3′), *lamp1* (*lamp1#2*, 5′-GGACATACACTCACTCTCAATTTCA-3′), and *lamp2* variants *2a* and *2b* (*lamp2#1*, 5′-TCAGGATAAGGTTGCTTCAGTTATT-3′; *lamp2#2*, 5′-GCAGCACCATTAAGTATCTAGACTT-3′) were from Invitrogen; siRNA targeting *mapk1* encoding for ERK2 (5′-UUAUCUGUUUCCAUGAGGUCC-3′) was from Ambion; and a control siRNA (5′-AAGGGATACCTAGACGTTCTA-3′) was from Dharmacon Research.

**Detection of cell viability and cell death.** Cell density was assessed by the 3-(4,5-dimethylthiazol-2-yl)-2,5-diphenyltetrazolium bromide (MTT; Sigma-Aldrich) reduction assay and cell death by lactate dehydrogenase (LDH) release assay (Roche) essentially as described previously (13). For the analysis of apoptosis-like cell death, cells were cotransfected with a plasmid encoding for a fusion protein consisting of histone 2B and enhanced green fluorescent protein (*H2B-eGFP-N1*; a gift from Christian Holmberg) and the indicated plasmid at a ratio of 1:10 using FuGENE-HD (Roche) according to the manufacturer's instructions. The percentage of green transfected cells with condensed nuclei was counted at an inverted fluorescence microscope (IX70, Olympus).

**Immunodetection and microscopy.** Immunoblotting and immunocytochemistry of formaldehyde-fixed cells were performed as described previously (24). Primary antibodies used included murine monoclonal antibodies against β-tubulin (clone E7), human LAMP-1 (clone H4A3), and human LAMP-2 (clone H4B4) from the Developmental Studies Hybridoma Bank (Department of Biological Sciences, University of Iowa, Iowa City, IA), H-Ras (clone 18) and human cathepsin L from BD Transduction Laboratories, human cathepsin L (clone 33/1; ref. 1) and human cathepsin B (clone AB-1) from Merck Chemicals, Src (clone EC10) from Millipore, ErbB2 (Ab-17) from Thermo Fisher Scientific, Inc., and glyceraldehyde-3-phosphate dehydrogenase (GAPDH) from Biogenesis; rat monoclonal antibodies against lysosomal $NH_2$ termini of LAMP-1 and LAMP-2 from the Developmental Studies Hybridoma Bank; rabbit monospecific antibody against phospho-p44/42 ERK (clone 197G2) from Cell Signaling Technology; polyclonal rabbit antiserum against cytosolic COOH terminus of LAMP-2 (lgp96) from Zymed/Invitrogen; as well as polyclonal goat antisera against ERK from Cell Signaling Technology and rat cathepsin B (3) and rat cathepsin L (clone S-20) from Santa Cruz Biotechnology, Inc. Appropriate peroxidase-conjugated secondary antibodies from DAKO A/S and Vector Laboratories were used for immunoblotting and the detection was accomplished using enhanced chemiluminescence Western blotting agents (Amersham Biosciences). The Image Gauge software v4.21 was used to quantify the protein levels. For immunocytochemistry, Alexa Fluor 576–conjugated or Alexa Fluor 488–conjugated secondary antibodies were used and fluorescence images were taken using a Zeiss Axiovert 100M laser scanning microscope.

Transmission electron microscopy was performed as described previously (28).

**Enzymatic activity measurements.** The total and cytoplasmic (digitonin extracted) cathepsin activities in NIH3T3 cells were measured in digitonin-treated samples using zFR-AFC (Enzyme System Products) probe as described previously (13, 24). The total cysteine cathepsin activities in Hkh2 and HCT116 cells were measured following extraction by freezing and thawing. *N*-acetyl-β-glucosamidase (NAG) activity was measured by incubating 2.5 volumes of NAG substrate solution [0.3 mg/mL 4-methylumbelliferyl *N*-acetyl-β-D-glucosaminide (Sigma-Aldrich) in 0.2 mol/L citrate buffer (pH 4.5)] with 1 volume of sample for 40 min at 37°C. To stop the reaction, two sample volumes of 0.2 mol/L glycine (pH 10.5, adjusted with NaOH) were added and the end point of substrate hydrolysis was analyzed (excitation, 455 nm; emission, 460 nm; and cutoff, 425 nm) using a SpectraMax Gemini flourometer (Molecular Devices). The acid phosphatase activity was measured after incubation of 1 volume of sample with 1 volume of 0.09 mol/L citrate buffer solution containing 2 mg/mL of 4-nitrophenyl phosphate disodium salt hexahydrate (Sigma-Aldrich) for 20 min at 25°C. The reaction was stopped by adding 4 volumes of 0.5 mol/L NaOH and the substrate hydrolysis was analyzed at 405 nm using a VersaMax tunable photospectrometer (Molecular Devices).

**Subcellular fractionation.** Equal amounts of cells were homogenized by 150 strokes in a DUALL glass homogenizer in a sucrose buffer [0.25 mol/L sucrose, 1 mmol/L EDTA, 20 mmol/L HEPES-NaOH (pH 7.4)] and centrifuged at 3,000 × *g* for 10 min. The supernatant containing the light membrane fraction (LMF) and cytoplasmic and microsomal fractions was subjected to a preestablished iodixanol gradient (24%-16%-10%-6%) and centrifuged at 50,000 × *g* for 17 h in an ultracentrifuge (rotor SW41Ti, 2331

Ultraspin 70, LKB Bromma). Fractions were carefully isolated from the gradient in 500 μL volumes and their density was analyzed by measuring the absorbance at 244 nm (Ultraspec 2000 spectrophotometer, Pharmacia Biotech).

**Analysis of mRNA.** RNA was harvested and analyzed by reverse transcription-PCR performed in the LightCycler 2.0 (Roche) with the FastStart SYBR Green I Master Mix (Roche) and appropriate primers (5′-CTTGCAAGGAGTGCGCTTGA-3′ and 5′-GCCTGGACCTGCACACTGAA-3′ for *lamp-1* and 5′-CACCCACTCCAACTCCAACT-3′ and 5′-GAACTTCCCA-GAGGGGCATC-3′ for *lamp-2*) at 500 nmol/L and the *lamp* expression in each sample was normalized to an external standard curve and evaluated relative to the porphobilinogen deaminase (*pbgd*) expression as described previously (29).

**Cloning of *lamp2*.** Murine *lamp2* variant *2* (NM_010685) cDNA was amplified by PCR from a cDNA library prepared from *pBabe-puro*–transduced NIH3T3 cells with appropriate primers (5′-CGAGGG-GATTCGTTGGAATTG-3′ and 5′-AGTGTTACAGAGTCTGATATCC-3′) and subcloned into the *Eco*RI site in *pBabe-puro*.

**Assays for lysosomal integrity.** Subconfluent U-2-OS cells incubated with 2 μg/mL acridine orange for 15 min at 37°C were washed, irradiated, and analyzed in HBSS complemented with 3% FCS. Cells for single-cell imaging were selected from eight predefined areas of each well in transmitted light mode, after which the same cells were immediately visualized and exposed to blue light from USH102 100 W mercury arc burner (Ushio Electric) installed in a U-ULS100HG housing (Olympus) for 20 s. Fluorescence microscopy was performed on Olympus IX70 inverted microscope with a LCPlanF1 ×20 objective with numerical aperture of 0.40. Loss of lysosomal pH gradient was quantified by counting the loss of intense red staining.

**Statistical analysis.** The statistical significance of the results was assessed using the unpaired or paired two-tailed *t* test in the case of two samples and the repeated measures or one-way ANOVA with the Dunnett's multiple comparisons post test (compare all versus control) in the case of more than two test samples.

## Results

**Transformation sensitizes cells to cathepsin-mediated cell death.** Immortalization of murine embryonic fibroblasts as well as their subsequent transformation by *v-H-ras* and *c-src*$^{Y527F}$ oncogenes sensitize them to cathepsin-mediated cell death induced by TNF and siramesine (17, 24). The same oncogenes have been reported to both sensitize and induce resistance to other cytotoxic agents (30–32). Thus, we tested the sensitivity of vector-transduced, *v-H-ras*–transduced, and *c-src*$^{Y527F}$–transduced NIH3T3 fibroblasts to cisplatin (alkylating agent that cross-links DNA), doxorubicin (anthracycline that intercalates DNA), and etoposide (topoisomerase II inhibitor). As shown in Fig. 1*A*, the *v-H-ras*– and *c-src*$^{Y527F}$–transduced cells exhibited significantly enhanced sensitivity to all the drugs tested. Akin to the TNF-induced death of the immortalized and transformed NIH3T3 fibroblasts (24), the death induced by the anticancer drugs was effectively inhibited by pharmacologic inhibitors of cysteine cathepsins [Ca-074-Me and z-Phe-Ala-fluoromethylketone (zFA-fmk)], whereas inhibitors of effector caspases (Asp-Glu-Val-Asp-chloromethylketone, DEVD-cmk, and DEVD-fmk) at concentrations up to 50 μmol/L were without an effect (Fig. 1*B*; data not shown).

These data suggest that these drugs induce a cathepsin-mediated caspase-independent cell death pathway in immortalized NIH3T3 cells that is further enhanced on transformation. Accordingly, cisplatin triggered 1.8 and 2.7 times more lysosomal leakage (measured as a percentage of cytosolic cathepsin activity of the total cathepsin activity) in the *v-H-ras*– and *c-src*$^{Y527F}$–transformed cells when compared with vector-transduced cells, respectively (Fig. 1*C*). Due to higher total levels of cathepsin activity in the transformed cells (see below), the actual cytosolic cysteine cathepsin activity was, in fact, ~4-fold higher in the cisplatin-treated transformed cells compared with vector-transduced cells (data not shown).

***v-H-ras* and *c-src*$^{Y527F}$ change the localization and density of lysosomes.** The ability of oncogenes to sensitize lysosomes to agents that trigger lysosomal membrane permeabilization by different signaling pathways suggested that the effect was due to their direct effect on lysosomes. To test this hypothesis, we costained vector-transduced, *v-H-ras*–transduced, and *c-src*$^{Y527F}$–transduced NIH3T3 fibroblasts with antibodies against LAMP-1 and Ras or Src. As reported earlier for oncogenic *ras* in breast epithelial cells (33), both *v-H-ras* and *c-src*$^{Y527F}$ had a pronounced effect on the distribution of the LAMP-1–positive vesicles in NIH3T3 cells (Fig. 2*A*). Whereas most LAMP-1–positive vesicles localized to the perinuclear region of the control cells, in transformed cells they were distributed throughout the cytosol, including the tips of the elongated filopodia in *v-H-ras*–transformed cells and invadopodia/podosomes in *c-src*$^{Y527F}$–transduced cells (Fig. 2*A* and *B*). Furthermore, H-Ras showed partial colocalization with LAMP-1 (Fig. 2*A*). This colocalization was biochemically verified by the analysis of LMFs obtained by iodixanol sucrose gradient centrifugation (Fig. 2*C*). H-Ras and, to a lesser extent, c-Src$^{Y527F}$ were enriched in the vesicle fractions containing the majority of LAMP-1, LAMP-2, and cathepsin B proteins as well as cysteine cathepsin activity (Fig. 2*C*). This analysis also revealed an oncogene-induced change in the density of cathepsin- and LAMP-containing vesicles, whereas the density of mitochondria, Golgi, and endoplasmic reticulum remained unchanged (Fig. 2*C*; Supplementary Fig. S1). In control cells, cysteine cathepsin activity peaked in fractions 12 and 13 (density, 1.065–1.069 g/mL), whereas in *v-H-Ras*– and *c-Src*$^{Y527F}$–transformed cells the activity was spread to fractions 10 to 15 (density, 1.049–1.07 g/mL) and 8 to 15 (density, 1.056–1.078 g/mL), respectively. The ratio of active cathepsin B to procathepsin B was increased in *v-H-Ras*– and *c-Src*$^{Y527F}$–transformed cells (Fig. 2*C*). 2*C*). Transmission electron microscopy of the cells showed a significant increase in large multilamellar bodies in both *v-H-Ras*– and *c-Src*$^{Y527F}$–transformed cells (Fig. 2*D*). Taken together, these data indicate that transformation by either *v-H-ras* or *c-src*$^{Y527F}$ changes the distribution, density, and ultrastructure of the endolysosomal compartment.

**Oncogenic transformation leads to cathepsin-dependent decrease in LAMP levels.** The highly homologous proteins LAMP-1 and LAMP-2 contribute to ~50% of all proteins of the lysosomal membrane (34, 35). They consist of a polypeptide core of ~40 kDa that forms a short cytoplasmic tail, a transmembrane domain, and a large intraluminal domain with extensive *N*-glycosylation and some *O*-glycosylation. The complex carbohydrate side chains contribute to up to 65% of the total molecular mass of LAMP-1 and LAMP-2, forming a nearly continuous coat on the inner surface of the lysosomal membrane. This carbohydrate coat has been suggested to serve as a barrier against the hydrolytic activity of the lysosomal enzymes. Interestingly, the analysis of vesicle fractions from vector-transduced, *v-H-ras*–transduced, and *c-src*$^{Y527F}$–transduced NIH3T3 fibroblasts suggested that the transformed cells had reduced levels of LAMP-1 and LAMP-2 proteins. To ensure that this was not due to the fractionation procedure, we analyzed their levels in total cell lysates. The data confirmed that transformation by *v-H-ras* and *c-src*$^{Y527F}$ dramatically decreased

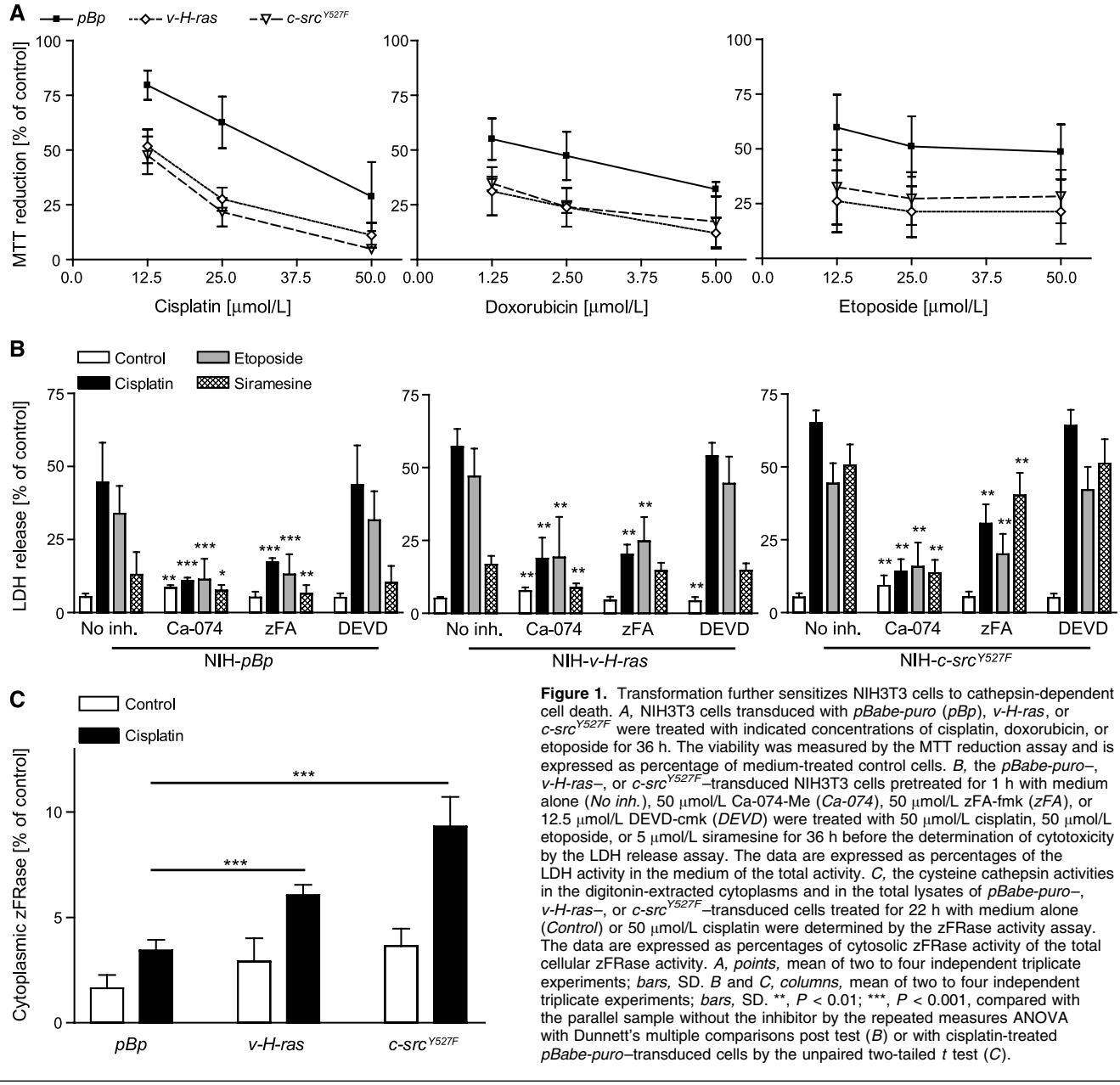


**Figure 1.** Transformation further sensitizes NIH3T3 cells to cathepsin-dependent cell death. *A,* NIH3T3 cells transduced with *pBabe-puro* (*pBp*), *v-H-ras*, or *c-src*$^{Y527F}$ were treated with indicated concentrations of cisplatin, doxorubicin, or etoposide for 36 h. The viability was measured by the MTT reduction assay and is expressed as percentage of medium-treated control cells. *B,* the *pBabe-puro*–, *v-H-ras*–, or *c-src*$^{Y527F}$–transduced NIH3T3 cells pretreated for 1 h with medium alone (*No inh.*), 50 μmol/L Ca-074-Me (*Ca-074*), 50 μmol/L zFA-fmk (*zFA*), or 12.5 μmol/L DEVD-cmk (*DEVD*) were treated with 50 μmol/L cisplatin, 50 μmol/L etoposide, or 5 μmol/L siramesine for 36 h before the determination of cytotoxicity by the LDH release assay. The data are expressed as percentages of the LDH activity in the medium of the total activity. *C,* the cysteine cathepsin activities in the digitonin-extracted cytoplasms and in the total lysates of *pBabe-puro*–, *v-H-ras*–, or *c-src*$^{Y527F}$–transduced cells treated for 22 h with medium alone (*Control*) or 50 μmol/L cisplatin were determined by the zFRase activity assay. The data are expressed as percentages of cytosolic zFRase activity of the total cellular zFRase activity. *A, points,* mean of two to four independent triplicate experiments; *bars,* SD. *B* and *C, columns,* mean of two to four independent triplicate experiments; *bars,* SD. **, $P < 0.01$; ***, $P < 0.001$, compared with the parallel sample without the inhibitor by the repeated measures ANOVA with Dunnett's multiple comparisons post test (*B*) or with cisplatin-treated *pBabe-puro*–transduced cells by the unpaired two-tailed *t* test (*C*).

the levels of both LAMP-1 and LAMP-2 in NIH3T3 fibroblasts (Fig. 3*A*). The reduction in LAMP-2 levels was observed by antibodies recognizing both the highly glycosylated lysosomal and the nonglycosylated cytosolic tails of the protein, indicating that the reduced immunoreactivity was not due to the increased glycosylation commonly observed in cancer cells (34). Notably, the *lamp1* and *lamp2* mRNA levels were equal in vector- and oncogene-transduced NIH3T3 cells, indicating that the transformation-associated regulation of LAMP-1 and LAMP-2 expression occurred at the posttranscriptional level (Fig. 3*B*). We have shown earlier that *v-H-ras* and *c-src*$^{Y527F}$ up-regulate the expression and activity of cysteine cathepsins B and L in NIH3T3 fibroblasts (24). Thus, we tested whether elevated cysteine cathepsin activity could be responsible for the enhanced turnover of LAMP-1 and LAMP-2. Indeed, the inhibition of cathepsins by compounds that raise the lysosomal pH (ConA and bafilomycin A) or by pharmaceutical cysteine cathepsin inhibitors [*N*-acetyl-leucyl-leucyl-norleucinal (ALLN), Ca-074-Me, and zFA-fmk] increased the levels of LAMPs in *v-H-ras*–transduced NIH3T3 fibroblasts ~2-fold (Fig. 3*C*; data not shown).

**The role of Raf-1-ERK pathway in the Ras-induced lysosomal changes.** Raf-1-ERK, Ral guanine nucleotide exchange factor (RalGEF), and phosphatidylinositol 3-kinase (PI3K) signaling pathways contribute to the Ras-mediated transformation (27). To investigate which pathway is responsible for the Ras-induced lysosomal effects in NIH3T3 fibroblasts, we took advantage of the dominantly active *H-ras-V12* effector loop mutants *35S, 37G*, and *40C* that preferentially activate Raf-1, RalGEF, and PI3K pathways,

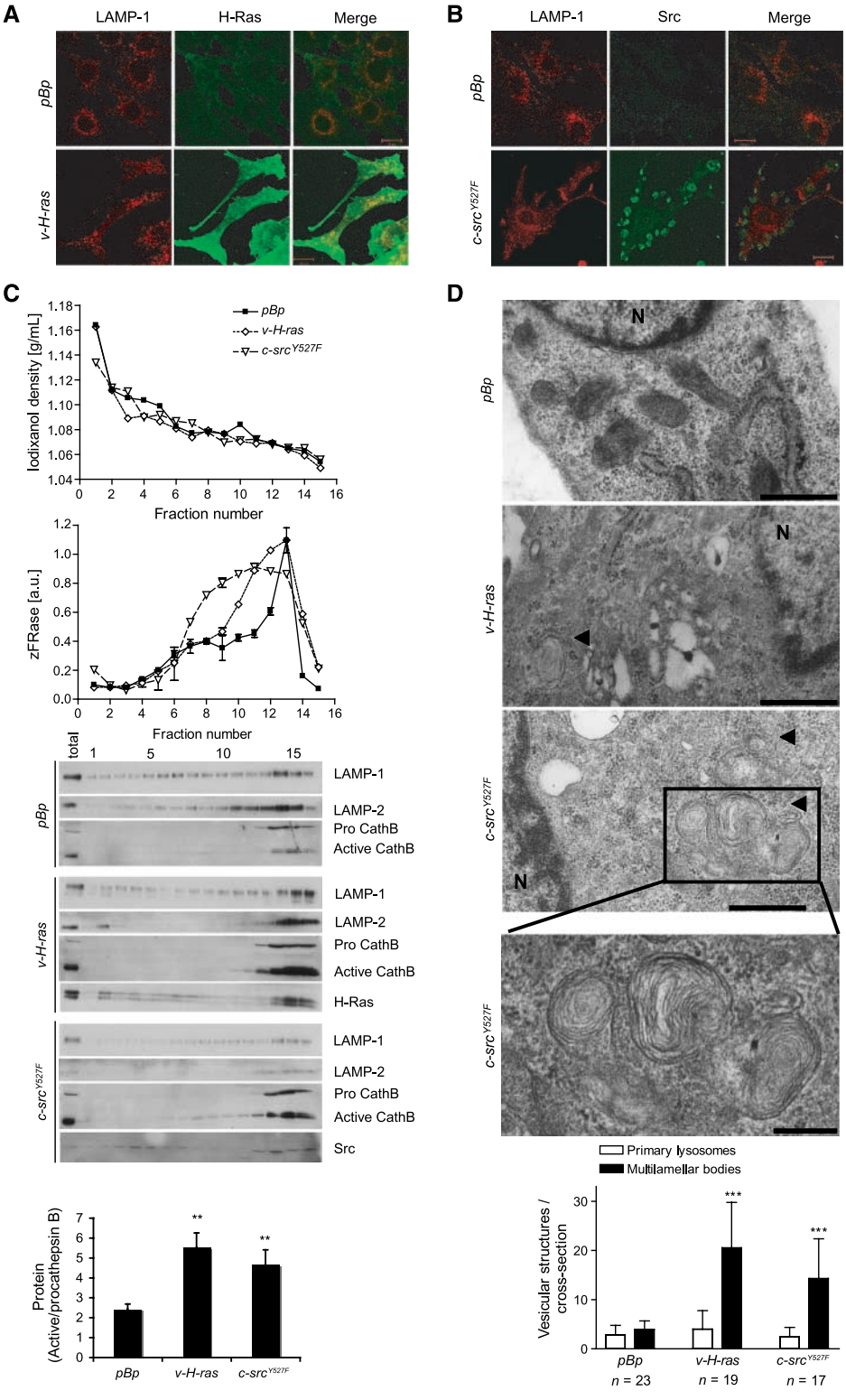


**Figure 2.** *v-H-ras* and *c-src*$^{Y527F}$ localize to lysosomes and alter lysosomal localization, density, and ultrastructure. *A* and *B,* representative confocal images of *pBabe-puro*–transduced, *v-H-ras*–transduced (*A*), and *c-src*$^{Y527F}$–transduced (*B*) NIH3T3 cells stained with indicated antibodies. *Scale bars,* 20 μm. *C,* the LMFs from indicated cell lines were subjected to iodixanol gradient centrifugation. The obtained fractions were analyzed for density (*top*), cysteine cathepsin activity (*middle*), and expression of indicated proteins (*bottom*). The inactive proform (*Pro*) and the mature active form (*Active*) of cathepsin B (*CathB*) are indicated. The experiment was performed twice with essentially same results. *Columns,* mean of ratios of active to proform of cathepsin B from three independent experiments; *bars,* SD. *AU,* arbitrary units. *D,* representative electron micrographs of *pBabe-puro*–, *v-H-ras*–, and *c-src*$^{Y527F}$–transduced NIH3T3 cells. *Scale bars,* 500 nm (*top, middle top*, and *middle bottom*) and 200 nm (*bottom*). *N,* nucleus. *Arrowheads,* multilamellar bodies. The histogram gives a semiquantitative analysis of primary lysosomes and multilamellar bodies in the cross-sections. *Columns,* mean; *bars,* SD. **, $P < 0.01$; ***, $P < 0.001$, compared with control cells by the unpaired two-tailed *t* test.

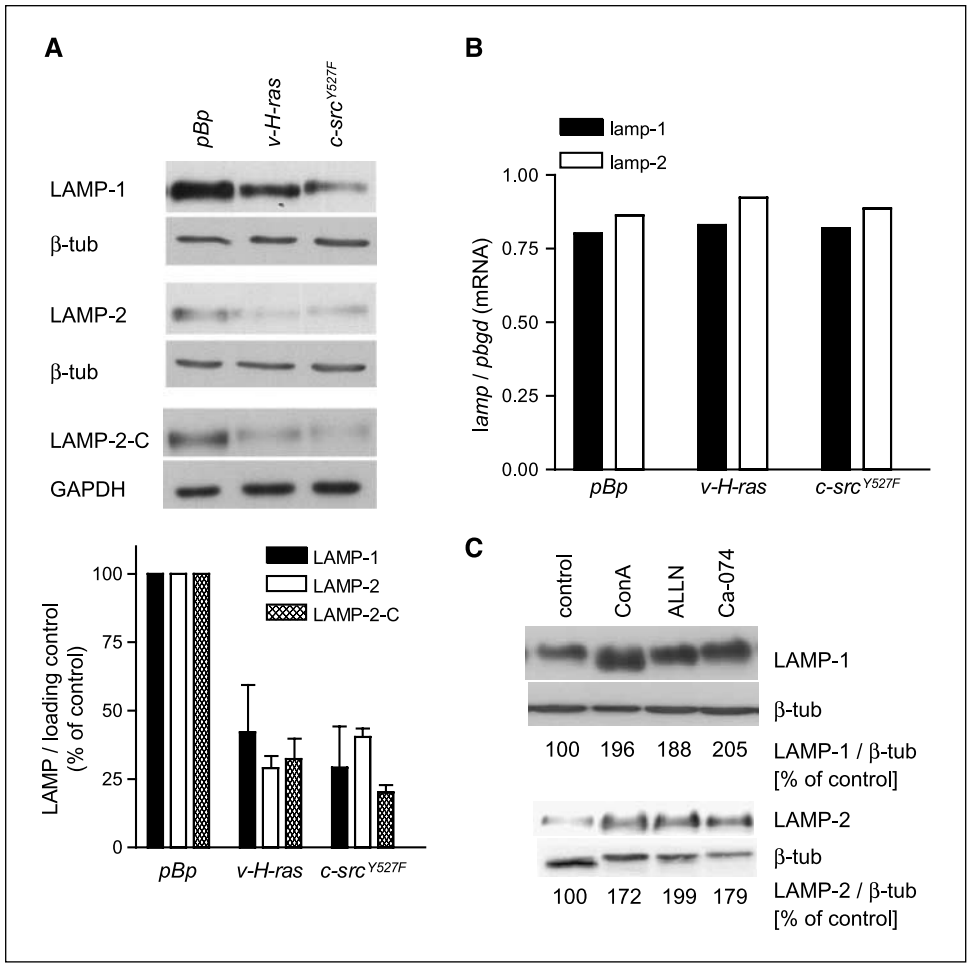


**Figure 3.** Oncogenic transformation induces a cathepsin-dependent decrease in LAMP-1 and LAMP-2 protein levels. *A,* representative immunoblots of proteins from *pBabe-puro–*, *v-H-ras–*, and *c-src*$^{Y527F}$–transduced NIH3T3 cells with antibodies against LAMP-1 (lysosomal, $NH_2$-terminal part), LAMP-2 (lysosomal, $NH_2$-terminal part), and LAMP-2-C (cytoplasmic, COOH-terminal part). β-Tubulin (*β-tub*) and GAPDH are shown as controls for equal loading. The values express the protein of interest to loading control ratios as percentages of those in *pBabe-puro*–transduced control cells. *Columns,* mean of three independent experiments; *bars,* SD. *B,* the mRNA levels of *lamp-1* and *lamp-2* were analyzed by real-time PCR. The data are presented relative to the level of the housekeeping gene *pdgd*. Averages of one triplicate experiment are shown. *C,* representative immunoblots of proteins from *v-H-ras*–transduced NIH3T3 cells left untreated (*Control*) or treated with 5 nmol/L ConA, 50 μmol/L ALLN, or 50 μmol/L Ca-074-Me for 20 h. The values express the LAMP to β-tubulin ratios as percentages of those in untreated control cells and represent means from three to five independent experiments.

respectively (27). Akin to *v-H-ras, H-ras-V12* increased the level of cysteine cathepsins and their activity, decreased the level of LAMP-1 and LAMP-2, and sensitized the cells to the cytotoxicity induced by cisplatin, etoposide, doxorubicin, and TNF (Fig. 4*A*–*C*). Contrary to the cysteine cathepsin activity, *v-H-ras* and *H-ras-V12* failed to affect the activity of two nonproteolytic lysosomal hydrolases: NAG and acid phosphatase (Fig. 4*B*). As reported previously (36), the *35S* effector loop mutant that activates the Raf-1-ERK pathway was sufficient to cause morphologic transformation comparable with that of *v-H-ras* and *H-ras-V12*, whereas *37G* and *40C* mutants had only a minimal transforming effect in NIH3T3 cells (data not shown). In concordance with the reported ability of the *35S* mutant to induce cathepsin L expression in NIH3T3 cells (36), it was also the only mutant that enhanced the expression of cathepsin B and the total activity of cysteine cathepsins as well as reduced the levels of LAMP-1 and LAMP-2 (Fig. 4*A* and *B*). The ability of pharmacologic inhibitors of the ERK pathway (U0126 and PD98059) to increase LAMP-2 protein levels and decrease cysteine cathepsin activity in *v-H-ras*–transformed cells further supported the involvement of the Raf-1-ERK pathway in Ras-mediated up-regulation of cathepsins and down-regulation of LAMPs (Fig. 4*A* and *B*). Importantly, the *H-ras-V12-35S* mutant sensitized NIH3T3 cells to the cytotoxicity induced by cisplatin, etoposide, doxorubicin, and TNF as effectively as *v-H-ras* and *H-ras-V12* (Fig. 4*C*). Notably, *37G* and *40C* mutants protected the NIH3T3 cells against TNF-induced cell death, whereas they had no effect on the cell death induced by the other agents. These data together with the data showing that U0126 and PD98059 effectively inhibited cisplatin- and etoposide-induced cell death in *v-H-ras*– and *c-src*$^{Y527F}$–transduced NIH3T3 fibroblasts (Fig. 4*D*; data not shown) indicate that the Raf-1-ERK pathway is primarily responsible for the oncogene-induced up-regulation of cysteine cathepsins, down-regulation of LAMP-2, as well as the increased sensitivity to the lysosomal cell death pathway in transformed NIH3T3 fibroblasts. The related mitogen-activated protein kinase pathways (c-Jun $NH_2$-terminal kinase and p38) are not likely to contribute to these lysosomal effects because their inhibitors (SB600125 and SB203580) failed to increase LAMP levels in *v-H-ras*–transformed cells (data not shown).

**Down-regulation of LAMPs is necessary, but not sufficient, to cell death sensitization.** To test whether the transformation-associated decrease in LAMP-1 and LAMP-2 levels was sufficient for the sensitization to the lysosomal cell death pathways, we transduced the NIH3T3 cells with two nonoverlapping short hairpin constructs targeting *lamp1* and two nonoverlapping short hairpins against the two splice variants of *lamp2*. All hairpins depleted the targeted proteins effectively, but the depletion of LAMP-1 was associated with an up-regulation of LAMP-2 and vice versa (Supplementary Fig. S1*A*). None of the hairpins had any effect on

the sensitivity of NIH3T3 cells to cisplatin (12.5–50 μmol/L), doxorubicin (1.25–5 μmol/L), etoposide (12.5–50 μmol/L), or TNF (0.01–1 ng/mL) plus cycloheximide (2.5 μmol/L) as analyzed by 16- to 21-h MTT reduction assays (data not shown). Furthermore, the depletion of neither *lamp1* nor *lamp2* had any apparent effect on cathepsin B expression (Supplementary Fig. S2*A*), cysteine cathepsin activity (zFRase), or lysosomal localization as analyzed by confocal microscopy (data not shown).

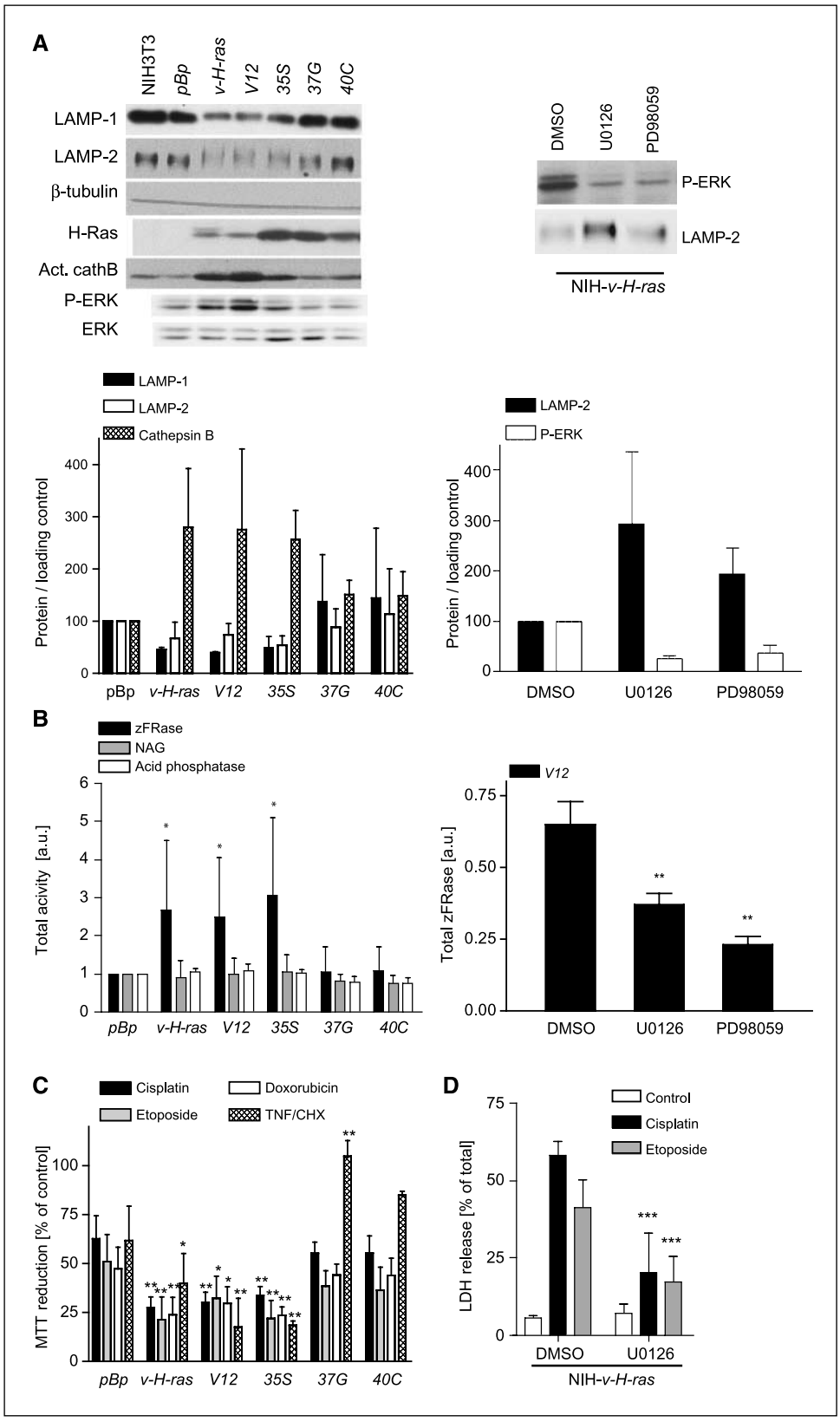


**Figure 4.** The Raf-1-ERK pathway mediates Ras-induced lysosomal changes. *A,* representative immunoblots of indicated proteins from parental NIH3T3 fibroblasts and NIH3T3 cells transduced with *pBabe-puro, v-H-ras, H-ras-V12* (*V12*), and Ras effector loop mutants activating the Raf-1-ERK (*35S*), Ral GDP dissociation stimulator (*37G*), and PI3K (*40C*) signaling pathways (*left*) and from *v-H-ras*–transduced cells treated for 68 h with DMSO, 50 μmol/L U0126, or 50 μmol/L PD98059 (*right*). The histograms below show the protein of interest to loading control (β-tubulin) ratios as percentages of those in *pBabe-puro*–transduced (*left*) or DMSO-treated (*right*) NIH3T3 cells. *Columns,* mean of three independent experiments; *bars,* SD. *B,* the activities of cysteine cathepsins (zFRase), NAG, and acid phosphatase were determined in total cell lysates from the cell lines described in *A* (*left*) and the zFRase activity was determined in lysates from *v-H-ras*–transduced cells treated as in *A*. The values on the left were normalized to the activities in *pBabe-puro*–transduced NIH3T3 cells. *Columns,* mean of three independent triplicate experiments; *bars,* SD. *C,* the cell lines listed in *A* were left untreated or treated with 25 μmol/L cisplatin, 25 μmol/L etoposide, or 2.5 μmol/L doxorubicin for 36 h or with 2.5 μmol/L cycloheximide (*CHX*) alone or with 0.1 ng/mL murine TNF for 20 h. The viability of cells was determined by the MTT reduction assay and is expressed as percentage of medium-treated control cells or cycloheximide-treated control cells (in the case of TNF/cycloheximide). *Columns,* mean of three independent triplicate experiments for anticancer drugs and one triplicate experiment for TNF/cycloheximide; *bars,* SD. *D,* the *v-H-ras*–transduced NIH3T3 cells treated for 20 h with DMSO or U0126 were treated with 50 μmol/L cisplatin or 50 μmol/L etoposide for 36 h before the determination of cytotoxicity by the LDH release assay. The data are expressed as percentages of the released LDH activity of the total activity. *Columns,* mean of four triplicate experiments; *bars,* SD. *, $P < 0.05$; **, $P < 0.01$; ***, $P < 0.001$, compared with similarly treated *pBabe-puro*–transduced control cells by the repeated measures and one-way (in the case of TNF/cycloheximide) ANOVA with the Dunnett's multiple comparisons post test (*B* and *C*).

To inhibit the compensatory up-regulation of the other *lamp*, we created cells with hairpins targeting both *lamp1* and *lamp2*. In spite of a depletion of both proteins comparable with that in oncogene-transformed cells (Fig. 3*A*; Supplementary Fig. S2*B*), these cells displayed unchanged sensitivity to lysosome-targeting cytotoxic compounds (Supplementary Fig. S2*C*). These data suggest that the down-regulation of LAMP-1 and LAMP-2 does not alone explain the enhanced sensitivity of transformed cells to the lysosomal cell death pathway. Therefore, we next tested whether the down-regulation of LAMPs was necessary for this phenomenon by transfecting the *v-H-ras*–transformed NIH3T3 fibroblasts with *lamp2* and a plasmid encoding for a fusion protein consisting of H2B and eGFP. In spite of a relatively small increase in LAMP-2 expression, the transfected cells were significantly protected against cisplatin-induced cell death compared with the vector-transfected cells (Fig. 5*A*). It should be noted that the ectopic expression of *lamp2* was associated with an elevated level of LAMP-1 in the transfected cells (Fig. 5*A*). These data suggest that the down-regulation of LAMPs is necessary for the oncogene-induced cell death–sensitive phenotype. The important role of LAMP-1 and LAMP-2 in lysosomal stability and cell survival in transformed cells was further supported by the ability of siRNAs against *lamp1* or *lamp2* to sensitize transformed cells (U-2-OS osteosarcoma) to cell death induced by the lysosome-destabilizing siramesine as well as to photo-oxidation–induced lysosomal destabilization (Fig. 5*B*–*D*).

**Oncogenes regulate LAMP-1 and LAMP-2 also in human carcinoma cells.** We next tested whether oncogenes also regulate the levels of LAMP-1 and LAMP-2 in human epithelial cells. For this purpose, we first compared human HCT116 colon carcinoma cells that express activated *K-ras* oncogene with HCT116-derived Hkh2 cells, in which the activated *K-ras* has been disrupted by homologous recombination (25). Akin to the murine fibroblast model system, *K-ras* sensitized HCT116 cells to cisplatin and siramesine (Fig. 6*A*), and as reported earlier, it enhanced the expression and activity of cysteine cathepsins (Fig. 6*B*; ref. 37). Furthermore, *K-ras* reduced the protein levels of LAMP-1 and LAMP-2 and resulted in their slower migration in the SDS-PAGE (Fig. 6*B*). This occurred in a cysteine cathepsin–dependent manner as shown by the ability of ConA and cysteine cathepsin inhibitors to significantly increase the level of LAMP-2 and its motility in SDS-PAGE in K-Ras–expressing HCT116 cells (Fig. 6*B*). Inhibition of ERKs by U0126 or PD98059 dramatically increased the expression of LAMP-2 and also slightly decreased their motility in SDS-PAGE in HCT116 cells, suggesting that the Raf-1-ERK signaling arm was also responsible for the oncogene-mediated down-regulation of LAMP proteins and change in their motility in this model system (Fig. 6*B*).

These results strongly suggest that the oncogene-mediated down-regulation of LAMP-1 and LAMP-2 as well as the sensitization to anticancer drugs are also relevant in human cancer cells. This view was further supported by the sensitization to cisplatin-induced cell death, increase in cathepsin expression, and reduction in the levels of LAMP-1 and LAMP-2 in MCF-7-tet-ΔNErbB2 breast carcinoma cells on induction of the expression of $NH_2$-terminally truncated active form of *erbb2* oncogene (*ΔNerbb2*) by the removal of tetracycline (Fig. 6*C* and *D*). Notably, *ΔNerbb2* induces a constitutive activation of ERKs in MCF-7 cells, and the inhibition of ERKs by U0126, PD98059, or siRNA-mediated depletion of *mapk1* that encodes for ERK2 increased the expression of LAMPs also in *ΔNerbb2*-expressing cells (Fig. 6*C* and *D*). Furthermore, the *ΔNerbb2*-induced down-regulation of LAMP1 was effectively reverted by siRNA-mediated depletion of *ctsb*, verifying the role of cysteine cathepsins in this process (Fig. 6*D*).

## Discussion

The data presented above show that transforming oncogenes induce a cysteine cathepsin–dependent reduction in LAMP protein levels and a significant sensitization to the lysosomal cell death pathways. Ectopic expression of *lamp2* in *v-H-ras*–transformed fibroblasts significantly reduced their sensitivity to cisplatin without affecting the level of cysteine cathepsins, indicating that the reduction in LAMP levels contributed to the observed cell death–sensitive phenotype. Whereas the depletion of *lamp1* or *lamp2* in human cancer cells destabilized their lysosomes and sensitized them to lysosome-destabilizing siramesine, effective depletion of *lamp1* and *lamp2* had no effect on the sensitivity of the nontransformed fibroblasts to the agents that trigger lysosomal leakage. Thus, other transformation-associated factors must act in concert with the reduced LAMP levels. The ability of the dominantly active *H-ras-V12* effector loop mutant *35S* to sensitize the cells to cytotoxic agents as effectively as the wild-type *H-ras-V12* and the sensitizing effect of pharmacologic inhibitors of the ERK pathway suggested that such factors are activated preferentially by the Raf-1-ERK signaling pathway. Thus, cysteine cathepsins, whose expression was also induced by *H-ras-V12-35S*, seem as obvious candidates. It is, however, technically impossible to test whether the increased cysteine cathepsin activity in transformed cells cooperates directly with decreased LAMP levels in destabilizing the lysosomes because experimental modulation of cathepsin activity also changes LAMP-1 and LAMP-2 levels.

Transformation-associated reduction in LAMP-1 and LAMP-2 levels seems to be mediated by cysteine cathepsin–mediated increase in the turnover of these proteins. First, the steady-state levels of *lamp-1* and *lamp-2* mRNAs were not affected by transformation. Second, inactivation of cysteine cathepsins by agents that increase the lysosomal pH, by pharmacologic inhibitors of cysteine cathepsins, and by RNA interference increased the level of LAMPs. Finally, both the increase in cysteine cathepsin expression and activity as well as the reduction in LAMP levels were mediated by the ERK signaling arm of *H-ras-V12*. It should be noted that also other lysosomal proteases can control the half-life of LAMP-1 and LAMP-2. For example, the deficiency or pharmacologic inhibition of cathepsin E, a lysosomal aspartic protease predominantly expressed in cells of the immune system, induces the accumulation of LAMP-1 and LAMP-2 in murine macrophages (39). Furthermore, cells defective in serine protease cathepsin A show reduced rates of LAMP-2a degradation (39). Thus, the cathepsin-mediated turnover of LAMPs and the subsequent sensitization to the lysosomal cell death might be a more universal phenomenon that is further enhanced on transformation. Interestingly, heat shock protein 70 (Hsp70) that effectively inhibits lysosomal membrane permeabilization is found on the inner membrane of lysosomes in some tumor cells (40). Thus, translocation of Hsp70 into the lysosomal membranes may present one of the mechanisms by which lysosomal membranes adapt to increased "cathepsin stress." Additionally, in the process of cancer progression, tumor cells may up-regulate the transcription of *lamp* mRNAs and thereby compensate for the deleterious effects of the reduced half-life of LAMP-1 and LAMP-2. This hypothesis is

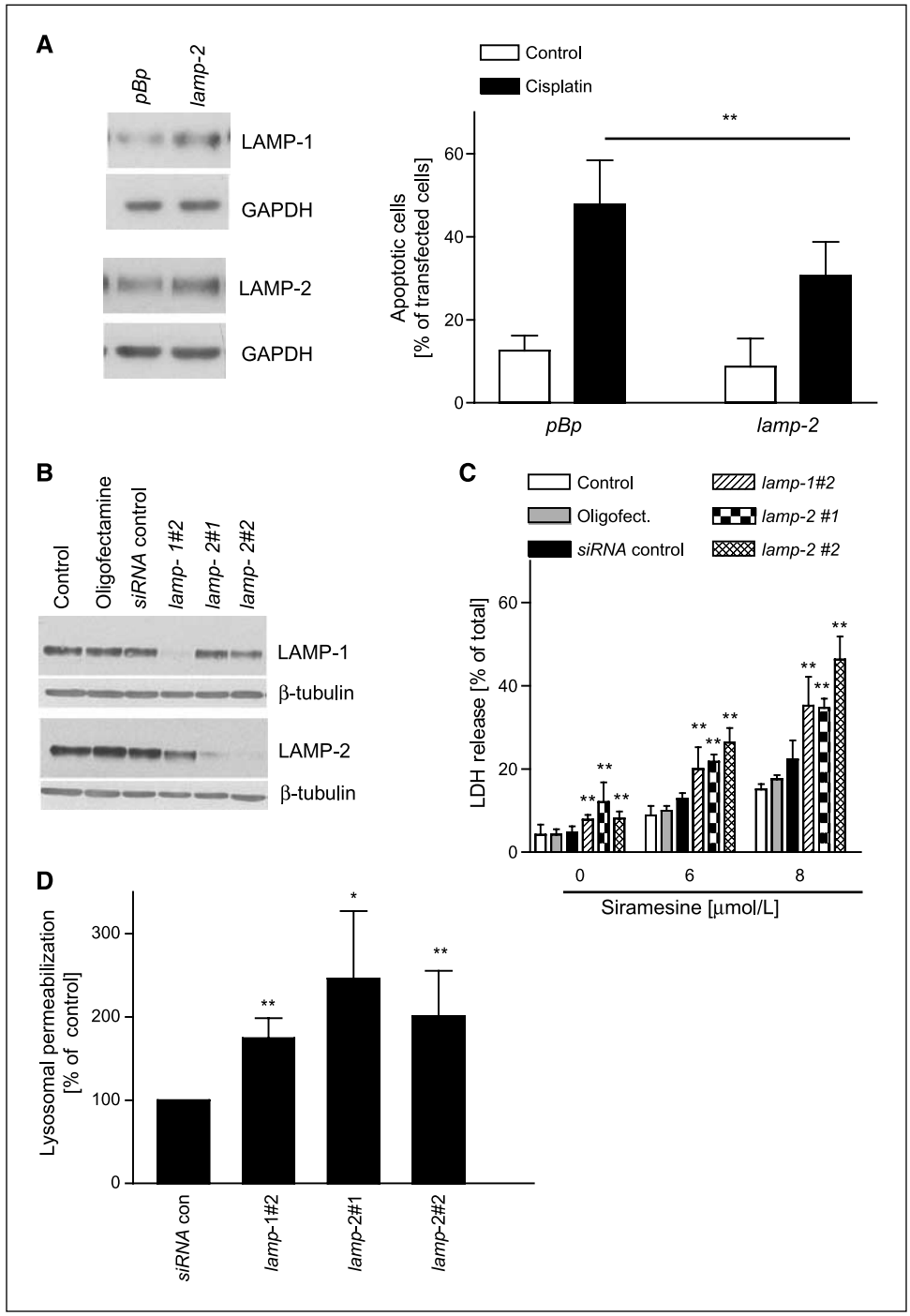


**Figure 5.** LAMP proteins protect cells from lysosomal cell death pathways. *A, left,* representative immunoblot analyses of LAMP-1 and LAMP-2 levels in *v-H-ras*–transduced NIH3T3 cells cotransfected with *H2B-eGFP-N1* and *pBabe-puro* or *pBabe-puro-Lamp-2* (*Lamp-2*) 24 h earlier are shown. The transfected cells were treated with 50 μmol/L cisplatin for 24 h starting 24 h after the transfection. The percentage of apoptotic cells was determined by counting the percentage of transfected green cells with condensed chromatin (using H2B-eGFP as a marker for transfection and for chromatin). *Columns,* average of eight independent fields; *bars,* SD. **, $P < 0.01$, compared with cisplatin-treated *pBabe-puro*–transduced cells by the unpaired two-tailed *t* test. *B,* representative immunoblots of indicated proteins from U-2-OS osteosarcoma cells left untreated (*Control*) or treated with Oligofectamine alone or together with control siRNA or siRNAs targeting *lamp-1* or *lamp-2* for 48 h. *C,* U-2-OS cells treated with indicated siRNAs for 56 h were treated with indicated concentrations of siramesine for additional 22 h before the determination of cytotoxicity by the LDH release assay. The data are expressed as percentages of the released LDH activity of the total activity. *Columns,* mean of three independent triplicate experiments; *bars,* SD. *D,* U-2-OS cells treated with indicated siRNAs for 24 h were labeled with 2 μg/mL acridine orange for 15 min, washed, and exposed to blue light for 20 s. Lysosomal permeabilization was evaluated as described in Materials and Methods. The data are expressed as percentages of the lysosomal permeabilization of siRNA control cells. *Columns,* mean of four independent experiments with 100 cells counted per condition; *bars,* SD. *, $P < 0.05$; **, $P < 0.01$, compared with untreated control cells by the repeated measures ANOVA with the Dunnett's multiple comparisons post test (*C*) and compared with control siRNA–treated cells by the paired two-tailed *t* test (*D*).

supported by studies showing increased levels of mRNAs for *lamp1* and *lamp2* as well as for another *lamp*, *lamp3*, in various human cancers (41, 42).

The transformation-associated changes in the lysosomal compartment were not limited to the increased cysteine cathepsin expression and reduced LAMP-1 and LAMP-2 levels. Lysosomes from transformed cells had a more dispersed localization within the cell and a much wider distribution in the density gradient when compared with lysosomes from vector-transduced control cells. Furthermore, transmission electron microscopy revealed a dramatic increase in multilamellar bodies and a decrease in the number of lysosomes with normal appearance. Interestingly, similar changes have been observed in the lysosomal compartment of *v-H-ras*–transformed melanocytes (43) as well as on up-regulation of cathepsin L expression (44). It remains to be studied whether the reduction in LAMP levels causes these changes in transformed cells. This idea is supported by the data showing that lysosomes from primary cells of *lamp1* and *lamp2* double-deficient mice are larger and more peripherally distributed and display multilamellar ultrastructure along with altered density (45).

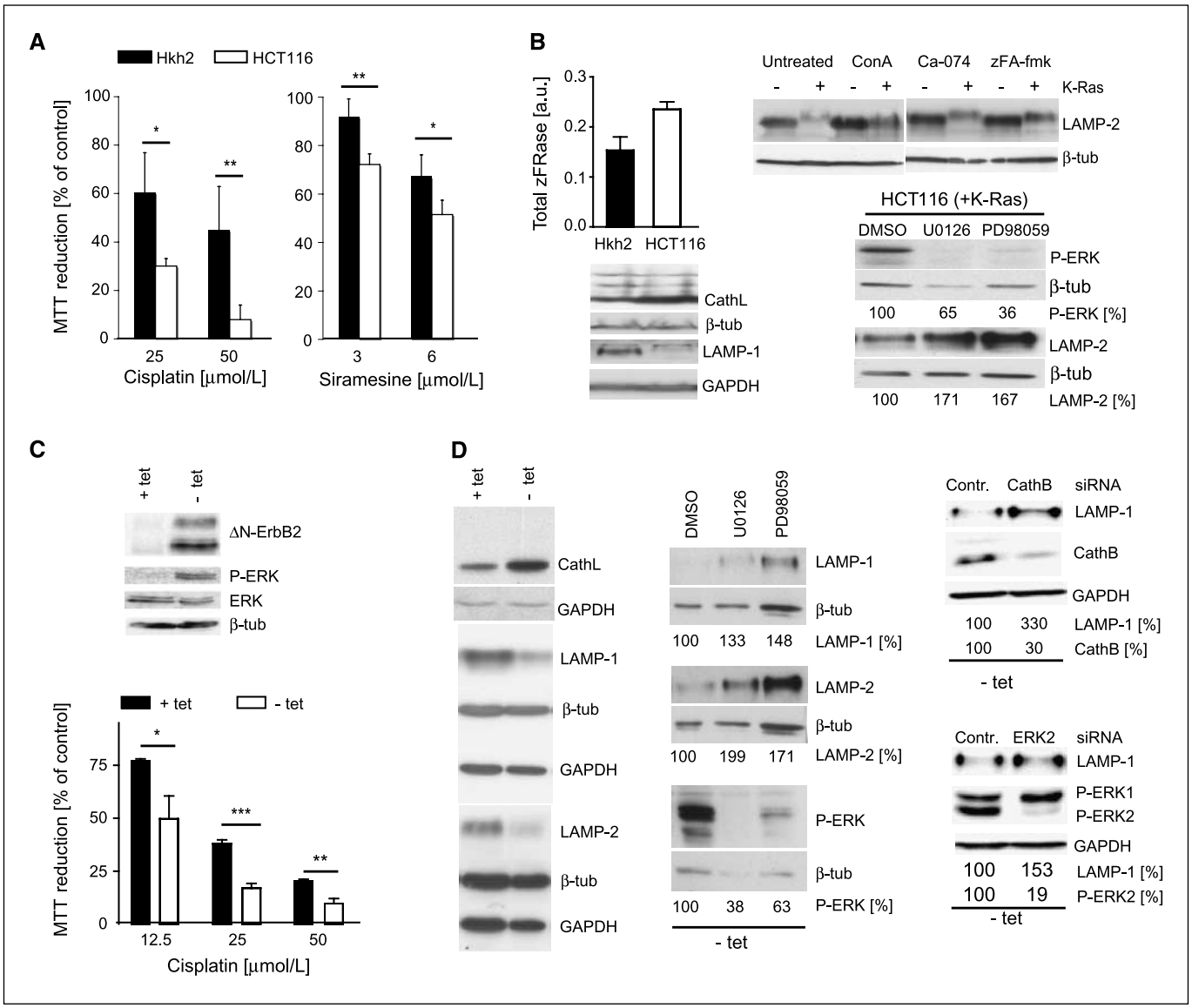


**Figure 6.** *K-ras* and *erbB2* up-regulate cathepsin L and down-regulate LAMPs in an ERK-dependent manner in human carcinoma cells. *A,* HCT116 and Hkh2 cells were treated with indicated concentrations of cisplatin or siramesine for 40 or 24 h, respectively. The cell viability was measured by the MTT reduction assay and is expressed as percentage of medium-treated control cells. *Columns,* average of four independent triplicate experiments; *bars,* SD. *, $P < 0.05$; **, $P < 0.01$, compared with similarly treated Hkh2 cells by the unpaired two-tailed *t* test. *B,* HCT116 (+K-Ras) and Hkh2 (−K-Ras) cells were analyzed for the total cysteine cathepsin activity (histogram) and for the levels of cathepsin L (*CathL*), LAMP-1, LAMP-2, phosphorylated ERK (*P-ERK*), and β-tubulin (loading control) by immunoblot analysis. When indicated, the cells were treated with 5 nmol/L ConA, 50 μmol/L Ca-074-Me, or 150 μmol/L zFA-fmk for 36 h or with DMSO vehicle control, 50 μmol/L U0126, or 50 μmol/L PD98059 for 72 h. *Columns,* mean cysteine cathepsin values from a triplicate experiment; *bars,* SD. The values express the protein of interest to loading control ratios as percentages of those in DMSO-treated control cells. All experiments were performed at least thrice with essentially same results. *C,* MCF-7-tet-ΔNErbB2 cells cultured in the presence (*+tet*) or absence (*−tet*; induction of *ΔNErbB2*) of tetracycline were analyzed for the expression of the indicated proteins by immunoblotting. The same cells were treated with indicated concentrations of cisplatin for 40 h and the cell viability was measured by the MTT reduction assay. *Columns,* mean of a triplicate experiment; *bars,* SD. The experiment was repeated twice with similar results. *, $P < 0.05$; **, $P < 0.01$; ***, $P < 0.001$, compared with similarly treated cells cultured in the presence of tetracycline by the unpaired two-tailed *t* test. *D,* representative immunoblots of indicated proteins from MCF-7-tet-ΔNErbB2 cells cultured in the presence (*+tet*) or absence (*−tet*) of tetracycline. When indicated, the cells were treated with DMSO vehicle, 50 μmol/L U0126, or 50 μmol/L PD98059 for 72 h or transfected with the indicated siRNAs 72 h before the lysis. The values express the protein of interest to loading control ratios as percentages of those in DMSO-treated control cells. The experiments were performed thrice with similar results.

Taken together, our data introduce cathepsin-mediated down-regulation of LAMP-1 and LAMP-2 as a mechanism by which various oncogenes sensitize cells to cytotoxic agents that trigger lysosomal membrane permeabilization. Although the increase in cysteine cathepsin activity has been well documented in metastatic tumors (6, 7), it remains to be shown whether LAMP-1 and LAMP-2 levels are concomitantly down-regulated in tumor tissue. Our data showing a K-Ras–mediated and cysteine cathepsin–mediated LAMP reduction in human colon carcinoma cells and ErbB2-mediated down-regulation of LAMPs in breast cancer cells suggest that this is the case at least in some tumors. These results strongly encourage the development of lysosome-targeting drugs for the treatment of highly metastatic cancers.

## Disclosure of Potential Conflicts of Interest

M. Jäättelä: Ownership interest, Lundbeck A/S. The other authors disclosed no potential conflicts of interest.

## Acknowledgments

Received 2/5/2008; revised 6/6/2008; accepted 6/11/2008.

**Grant support:** Danish Cancer Society, Danish National Research Foundation, Danish Medical Research Council, Association for International Cancer Research, Meyer Foundation, Vilhelm Pedersen Foundation, M.L Jørgensen and Gunnar Hansens Foundation, Novo Nordisk Foundation, and Danish Cancer Research Foundation.

The costs of publication of this article were defrayed in part by the payment of page charges. This article must therefore be hereby marked *advertisement* in accordance with 18 U.S.C. Section 1734 solely to indicate this fact.

We thank K. Grøn Henriksen, P. Rammer, T. Chaaban, M. Daugaard, and J. Hinrichsen for technical assistance; S. Courtneidge, Channing Der, N. Dietrich, Christian Holmberg, Christian Thomsen, J. Thastrup, and P. Szyniarowski for providing invaluable research tools; and J. August, J. Hildreth, and M. Klymkowsky for the development of hybridomas or monoclonal antibodies obtained from the Developmental Studies Hybridoma Bank developed under auspices of the National Institute of Child Health and Human Resources and maintained by The University of Iowa.

## References

1. Eskelinen EL, Tanaka Y, Saftig P. At the acidic edge: emerging functions for lysosomal membrane proteins. Trends Cell Biol 2003;13:137–45.
2. Luzio JP, Pryor PR, Bright NA. Lysosomes: fusion and function. Nat Rev Mol Cell Biol 2007;8:622–32.
3. de Duve C. The lysosome turns fifty. Nat Cell Biol 2005;7:847–9.
4. Kroemer G, Jäättelä M. Lysosomes and autophagy in cell death control. Nat Rev Cancer 2005;5:886–97.
5. Turk V, Turk B, Turk D. Lysosomal cysteine proteases: facts and opportunities. EMBO J 2001;20:4629–33.
6. Sloane BF, Yan S, Podgorski I, et al. Cathepsin B and tumor proteolysis: contribution of the tumor microenvironment. Semin Cancer Biol 2005;15:149–57.
7. Joyce JA, Hanahan D. Multiple roles for cysteine cathepsins in cancer. Cell Cycle 2004;3:1516–619.
8. Gocheva V, Zeng W, Ke D, et al. Distinct roles for cysteine cathepsin genes in multistage tumorigenesis. Genes Dev 2006;20:543–56.
9. Guicciardi ME, Leist M, Gores GJ. Lysosomes in cell death. Oncogene 2004;23:2881–90.
10. Hanahan D, Weinberg RA. The hallmarks of cancer. Cell 2000;100:57–70.
11. Jäättelä M. Multiple cell death pathways as regulators of tumour initiation and progression. Oncogene 2004;23:2746–56.
12. Brunk UT, Svensson I. Oxidative stress, growth factor starvation and Fas activation may all cause apoptosis through lysosomal leak. Redox Rep 1999;4:3–11.
13. Foghsgaard L, Wissing D, Mauch D, et al. Cathepsin B acts as a dominant execution protease in tumor cell apoptosis induced by tumor necrosis factor. J Cell Biol 2001;153:999–1009.
14. Yuan XM, Li W, Dalen H, et al. Lysosomal destabilization in p53-induced apoptosis. Proc Natl Acad Sci U S A 2002;99:6286–91.
15. Bidere N, Lorenzo HK, Carmona S, et al. Cathepsin D triggers Bax activation, resulting in selective AIF relocation in T lymphocytes entering the early commitment phase to apoptosis. J Biol Chem 2003;278:31401–11.
16. Broker LE, Huisman C, Span SW, Rodriguez JA, Kruyt FA, Giaccone G. Cathepsin B mediates caspase-independent cell death induced by microtubule stabilizing agents in non-small cell lung cancer cells. Cancer Res 2004;64:27–30.
17. Ostenfeld MS, Fehrenbacher N, Høyer-Hansen M, Thomsen C, Farkas T, Jäättelä M. Effective tumor cell death by σ-2 receptor ligand siramesine involves lysosomal leakage and oxidative stress. Cancer Res 2005;65:8975–83.
18. Gyrd-Hansen M, Farkas T, Fehrenbacher N, et al. Apoptosome-independent activation of lysosomal cell death pathway by caspase-9. Mol Cell Biol 2006;26:7880–91.
19. Groth-Pedersen L, Ostenfeld M, Høyer-Hansen M, Nylandsted J, Jäättelä M. Vincristine induces dramatic lysosomal changes and sensitizes cancer cells to lysosome destabilizing siramesine. Cancer Res 2007;67:2217–25.
20. Cirman T, Oresic K, Droga Mazovec G, et al. Selective disruption of lysosomes in HeLa cells triggers apoptosis, mediated by cleavage of Bid by multiple papain-like lysosomal cathepsins. J Biol Chem 2004;279:3578–87.
21. Leist M, Jäättelä M. Four deaths and a funeral: from caspases to alternative mechanisms. Nat Rev Mol Cell Biol 2001;2:589–98.
22. Ostenfeld MS, Hoyer-Hansen M, Bastholm L, et al. Anti-cancer agent siramesine is a lysosomotropic detergent that induces cytoprotective autophagosome accumulation. Autophagy 2008;4:487–99.
23. Brunk UT, Neuzil J, Eaton JW. Lysosomal involvement in apoptosis. Redox Rep 2001;6:91–7.
24. Fehrenbacher N, Gyrd-Hansen M, Poulsen B, et al. Sensitization to the lysosomal cell death pathway upon immortalization and transformation. Cancer Res 2004;64:5301–10.
25. Ohmori M, Shirasawa S, Furuse M, Okumura K, Sasazuki T. Activated Ki-ras enhances sensitivity of ceramide-induced apoptosis without c-Jun $NH_2$-terminal kinase/stress-activated protein kinase or extracellular signal-regulated kinase activation in human colon cancer cells. Cancer Res 1997;57:4714–7.
26. Egeblad M, Mortensen OH, Jäättelä M. Truncated ErbB2 receptor enhances ErbB1 signaling and induces reversible, ERK-independent loss of epithelial morphology. Int J Cancer 2001;94:185–91.
27. Khosravi-Far R, White MA, Westwick JK, et al. Oncogenic Ras activation of Raf/mitogen-activated protein kinase-independent pathways is sufficient to cause tumorigenic transformation. Mol Cell Biol 1996;16:3923–33.
28. Nylandsted J, Rohde M, Brand K, Bastholm L, Elling F, Jäättelä M. Selective depletion of heat shock protein 70 (Hsp70) activates a tumor-specific death program that is independent of caspases and bypasses Bcl-2. Proc Natl Acad Sci U S A 2000;97:7871–6.
29. Rohde M, Daugaard M, Jensen MH, Helin K, Nylandsted J, Jäättelä M. Members of the heat-shock protein 70 family promote cancer cell growth by distinct mechanisms. Genes Dev 2005;19:570–82.
30. Peters GJ, Wets M, Keepers YP, et al. Transformation of mouse fibroblasts with the oncogenes H-ras or trk is associated with pronounced changes in drug sensitivity and metabolism. Int J Cancer 1993;54:450–5.
31. Basu A, Cline JS. Oncogenic transformation alters cisplatin-induced apoptosis in rat embryo fibroblasts. Int J Cancer 1995;63:597–603.
32. Chen G, Shu J, Stacey DW. Oncogenic transformation potentiates apoptosis, S-phase arrest and stress-kinase activation by etoposide. Oncogene 1997;15:1643–51.
33. Nishimura Y, Sameni M, Sloane BF. Malignant transformation alters intracellular trafficking of lysosomal cathepsin D in human breast epithelial cells. Pathol Oncol Res 1998;4:283–96.
34. Fukuda M. Lysosomal membrane glycoproteins. Structure, biosynthesis, and intracellular trafficking. J Biol Chem 1991;266:21327–30.
35. Eskelinen EL. Roles of LAMP-1 and LAMP-2 in lysosome biogenesis and autophagy. Mol Aspects Med 2006;27:495–502.
36. Collette J, Ulku AS, Der CJ, Jones A, Erickson AH. Enhanced cathepsin L expression is mediated by different Ras effector pathways in fibroblasts and epithelial cells. Int J Cancer 2004;112:190–9.
37. Cavallo-Medved D, Dosescu J, Linebaugh BE, Sameni M, Rudy D, Sloane BF. Mutant K-ras regulates cathepsin B localization on the surface of human colorectal carcinoma cells. Neoplasia 2003;5:507–19.
38. Yanagawa M, Tsukuba T, Nishioku T, et al. Cathepsin E deficiency induces a novel form of lysosomal storage disorder showing the accumulation of lysosomal membrane sialoglycoproteins and the elevation of lysosomal pH in macrophages. J Biol Chem 2007;282:1851–62.
39. Cuervo AM, Mann L, Bonten EJ, d'Azzo A, Dice JF. Cathepsin A regulates chaperone-mediated autophagy through cleavage of the lysosomal receptor. EMBO J 2003;22:47–59.
40. Nylandsted J, Gyrd-Hansen M, Danielewicz A, et al. Heat shock protein 70 promotes cell survival by inhibiting lysosomal membrane permeabilization. J Exp Med 2004;200:425–35.
41. Furuta K, Ikeda M, Nakayama Y, et al. Expression of lysosome-associated membrane proteins in human colorectal neoplasms and inflammatory diseases. Am J Pathol 2001;159:449–55.
42. Ozaki K, Nagata M, Suzuki M, et al. Isolation and characterization of a novel human lung-specific gene homologous to lysosomal membrane glycoproteins 1 and 2: significantly increased expression in cancers of various tissues. Cancer Res 1998;58:3499–503.
43. Donatien PD, Diment SL, Boissy RE, Orlow SJ. Melanosomal and lysosomal alterations in murine melanocytes following transfection with the v-rasHa oncogene. Int J Cancer 1996;66:557–63.
44. Collette J, Bocock JP, Ahn K, et al. Biosynthesis and alternate targeting of the lysosomal cysteine protease cathepsin L. Int Rev Cytol 2004;241:1–51.
45. Eskelinen EL, Schmidt CK, Neu S, et al. Disturbed cholesterol traffic but normal proteolytic function in LAMP-1/LAMP-2 double-deficient fibroblasts. Mol Biol Cell 2004;15:3132–45.